Research on the Constitutive Model of New Hybrid Fiber ECC under Compression

Lijian Zhou, Liguang Xu*, Rui Zhang, Hua Deng

School of Civil Engineering and Architecture, Northeast Petroleum University, Daqing, Heilongjiang, 163318, China

*E-mail: 1635536292@qq.com

Abstract. To optimize the fiber mix ratio and simplify the compressive constitutive model, thereby enhancing the practicality of Engineered Cementitious Composite (ECC) materials, this study conducts an analysis through uniaxial compression experiments. The experiments combine both macro and micro perspectives to observe the cross-section and analyze the effects of fiber length and replacement ratio on the compressive strength of ECC materials. The results indicate that the addition of POM fibers can improve the dispersion of PVA fibers, leading to enhanced compressive performance; the toughness index increases with the fiber length. When the replacement ratio is at 50%, the impact of fiber length on the material's toughness is minimal. Finally, based on the stress-strain curves obtained from the experiments, a recommended model for the compressive stress-strain curve is proposed.

Keywords: Fiber hybridization; Compression parameters; Stress-strain curve model

1 Introduction

Engineered Cementitious Composites (ECC) exhibit high ductility and exceptional crack resistance, making them promising candidates for applications in building repair and reinforcement. Various types of fibers, such as polymer, steel, and carbon fibers, are typically employed to enhance their properties, yielding high extensibility with maximum strain capacities ranging from 3% to 5%[1].In practical applications, cement-based materials must possess adequate compressive strength; however, the limited understanding of the compressive properties of ECC hinders its widespread structural use.

Therefore, elucidating the compressive behavior of ECC and establishing a constitutive model for its stress-strain relationship is of great significance. Zhou et al.[2]described the compressive behavior of ECC with compressive strength ranging from 35 to 60 MPa and proposed a constitutive model that considers the localization features in the post-peak phase of ECC. However, the applicability and generality of this model have not been extensively discussed. Polyvinyl alcohol (PVA) fibers are commonly used in the production of ECC materials and offer clear advantages in

© The Author(s) 2025
Y. Zhang et al. (eds.), *Proceedings of the 2024 10th International Conference on Architectural, Civil and Hydraulic Engineering (ICACHE 2024)*, Advances in Engineering Research 259,
https://doi.org/10.2991/978-94-6463-658-1_55

practical engineering applications. Nevertheless, challenges such as high cost and poor dispersion remain. To leverage the superior properties of PVA fibers while addressing their limitations, many researchers have incorporated other fibers into the mix. LOH et al.[3]found that fiber hybridization can enhance the ductility of the material. Zhang et al.[4]demonstrated through experiments that steel-PVA hybrid fibers could improve compressive performance while optimizing the fiber proportion to reduce costs. Co-polymerized formaldehyde (POM) fibers exhibit advantages such as easy dispersion, high alkali resistance, and low-temperature durability, making them suitable for the preparation of Engineered Cementitious Composites (ECC). Notably, the cost of POM fibers is only one-sixth that of PVA fibers; however, there is currently limited research on this material.

Therefore, this study employs five different replacement ratios and three fiber lengths to investigate the effects of replacement ratio and fiber length on the compressive performance of ECC. Additionally, a recommended model for the stress-strain curve is provided, aiming to develop a cost-effective and practical new type of ECC material.

2 Experiment

As structural materials in compression zones, cement-based materials exhibit crucial compressive strength. To achieve optimal experimental results, this study determined the material proportions through multiple trials. A total of 13 groups were established, incorporating five fiber replacement rates (0%, 25%, 50%, 75%, and 100%), with 12 mm long PVA fibers and POM fibers of three different lengths (8 mm, 12 mm, and 16 mm) (details in Table 2). Standard 100 mm × 100 mm × 100 mm specimens were prepared and cured for 28 days before testing (as shown in Figure 1). The mix proportions of the benchmark cement-based composite materials are presented in Table 1.

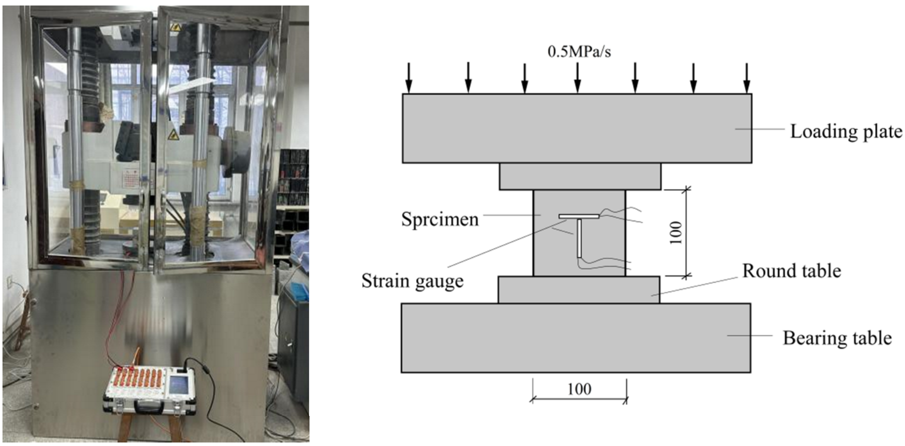

(a)Experimental equipment (b)Loading condition

Fig. 1. compression test (unit: mm)

Table 1. Mix ratio of reference cement-based material

Mixing ratio/kg·m^{-3}					Water reducer/%	Water-to-gel ratio	Fiber Volume Ratio/%
Cement	Fly ash	Silica fume	Water	quartz sand			
1000	900	100	480	720	0.3	0.24	2.0

Table 2. Fiber Ratio Design

Number	Replacement rate/%	Length of POM fiber/mm
A2	0	——
E1	25	8
E2	25	12
E3	25	16
D1	50	8
D2	50	12
D3	50	16
C1	75	8
C2	75	12
C3	75	16
B1	100	8
B2	100	12
B3	100	16

3 Results and Discussion

3.1 Experimental Data

As shown in Table 3, the fiber replacement ratio and fiber length significantly affect the compressive strength of the material. Under an appropriate fiber combination, the two types of fibers interweave, thereby delaying crack propagation to varying degrees and compensating for the limitations of single fibers in enhancing material properties. In contrast, an improper fiber ratio can lead to uneven fiber distribution, resulting in increased porosity and reduced compressive strength. The compressive strength of Group E3 increased by 7.37% compared to Group A2, while Group C2 exhibited an 8.02% decrease relative to Group A2.

Table 3. Compression test data

Number	f_c/MPa	E_0/GPa	v_0	ε_0/%
A2	66.62	22.7	0.23	0.3549
E1	66.02	23.6	0.23	0.4467
E2	64.21	19.2	0.23	0.3425
E3	71.53	20.9	0.22	0.3545
D1	70.26	20.7	0.22	0.4602

D2	63.86	22.9	0.23	0.3180
D3	67.33	25.5	0.24	0.3644
C1	65.30	17.9	0.23	0.4479
C2	61.28	18.7	0.24	0.3394
C3	65.56	24.9	0.23	0.3765
B1	57.22	17.7	0.24	0.2740
B2	59.18	17.9	0.25	0.3059
B3	64.96	22.6	0.23	0.3295

where f_c represents the peak stress; ε_0 represents the strain at the peak load; E_0 is the modulus of elasticity; and v_0 is the Poisson's ratio.

3.2 Destructive Pattern

3.2.1 Macro-Destructive Pattern.

Fibers serve as obstacles to crack propagation within the matrix, continuously dissipating and distributing stress, thereby limiting the size of the specimens and preventing overall failure. As the load increases, the bridging effect of the fibers is progressively activated, exerting multidirectional constraints on the specimens. Examination of the failure modes reveals that the failure pattern of Group A2 is particularly distinctive, characterized by the delamination of the surface layer from the core, resulting in flaking (see Figure 2a). This may be attributed to poor distribution of the PVA fibers in this mix. In contrast, the failure mode of the hybrid fiber ECC under compression demonstrates greater toughness compared to the single-fiber group, with an increased number of cracks that are narrower in width. Additionally, there were no signs of extensive surface flaking or total collapse, indicating that the inclusion of POM fibers improved the distribution of PVA fibers (see Figure 2b).

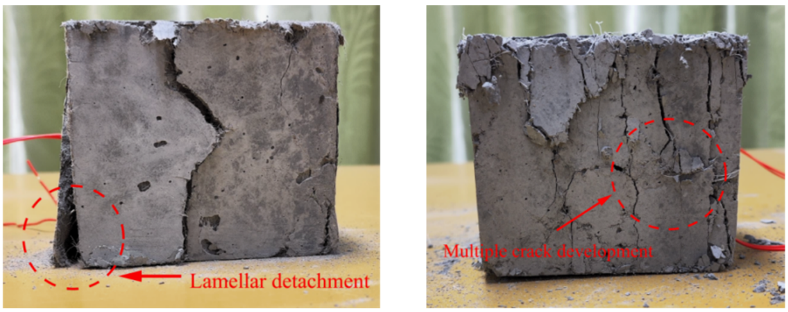

(a)Failure pattern of group A2 (b)Damage pattern of hybrid fiber group

Fig. 2. Failure mode under compressive load

3.2.2 Micro-Destruction Pattern.

To investigate the causes of macro-scale failure modes and validate the proposed hypothesis, a digital microscope was employed to examine the fiber distribution on the fracture surfaces of the specimens after compression, as shown in Figure 3. As illustrated in Figure 3a, despite efforts to disperse the PVA fibers as much as possible before the experiment, a phenomenon of fiber agglomeration was still evident, particularly pronounced in Group A2. Localized fiber clumping resulted in a decrease in cement material density in those areas. Consequently, most of the C-S-H gel and ettringite generated during the hydration of the gel material adhered to the highly concentrated PVA fibers, weakening the connections between the ettringite crystals. This ultimately led to a reduction in load-bearing capacity, adversely affecting the material's performance. The analysis indicates that the agglomeration of PVA fibers results in strong bonding within the fiber clusters, while weak points emerge between the clusters, leading to the detachment of large sections.

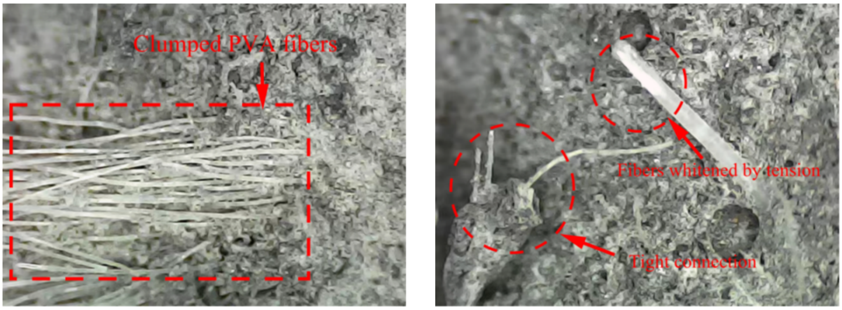

(a) Clumped PVA fibers (b)The two fibers work together

Fig. 3. The condition of the fibers on the cross section

Observation of the groups with higher compressive strength, as shown in Figure 3b, reveals that the incorporation of POM fibers optimizes the distribution of PVA fibers. The fine, soft PVA fibers compensate for the issues caused by the larger air bubbles associated with POM fibers. The random orientation and interconnection of these two types of fibers create a multiphase structure within the cement gel, enhancing the ability to disperse and absorb stress under loading conditions. Additionally, the pullout or breakage of the fibers further dissipates energy, resulting in an overall increase in compressive strength. It is also noted that the tips of the fibers appear white due to tension, indicating that their properties are fully utilized before fracture. Many fibers in the fracture surface are connected to shattered gel material particles. As cracks develop in the specimens under load, the fibers consume fracture energy through pullout or breakage, significantly contributing to the prevention of sudden failure in the brittle cement-based materials.

3.3 Toughness Index

The Toughness Index (TI) is a crucial parameter for characterizing the energy absorption capacity and ductility of materials. TI is defined as the ratio of the area under the stress-strain curve below $3\varepsilon_0$ to the area below ε_0 (see Figure 4a)[5]. Based on this definition, Figure 4b illustrates the effects of fiber replacement ratio and fiber length on the TI value. As shown in Figure 4b, there is a noticeable trend of increasing TI with longer fiber lengths, indicating that longer fibers are more effective at forming a three-dimensional network structure, which efficiently disperses stress and enhances the lateral tensile capacity of the material. This characteristic helps to prevent premature cracking due to insufficient tensile load-bearing capacity, thereby increasing the material's ductility. In contrast, shorter fibers tend to provide more localized reinforcement. Additionally, it can be observed that at a fiber replacement ratio of 50%, the TI values of samples with three different fiber lengths (8 mm, 12 mm, and 16 mm) are relatively close, suggesting that fiber length has a minimal impact on material ductility at this replacement ratio.

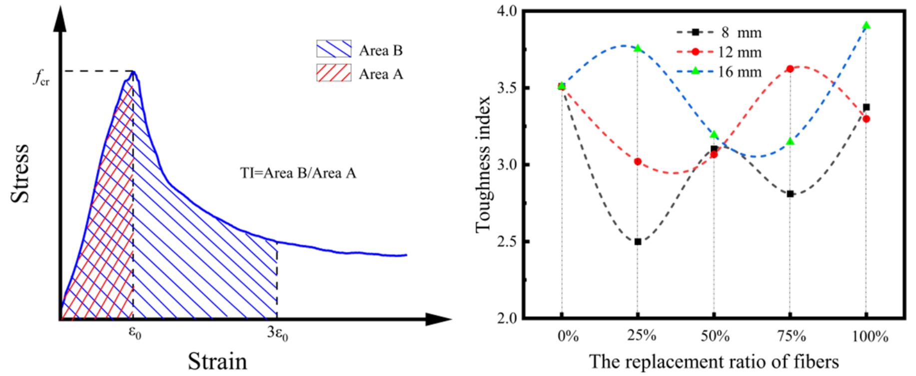

(a) Definition of TI (b)Compressive toughness coefficient of each group

Fig. 4. Definition of TI and TI in each group of ECC

3.4 Constitutive Model

To describe the failure process under uniaxial compression, the full stress-strain curve model is essential for structural nonlinear analysis. The stress-strain curve can be simplified through normalization, where the x-axis represents the normalized strain, defined as $\epsilon/\epsilon cu\epsilon/\epsilon cu$, and the y-axis represents the normalized stress, defined as σ/f_c. Therefore, the vertex of the normalized stress-strain curve is located at the coordinates (1, 1). Numerous studies have been conducted on this topic, and the following section will compare four widely used models with experimental results (using Group C as an example).

The first model is the one proposed by Wang et al.[6], who derived the concrete stress-strain curve expression experimentally, as shown in Equation (1). This model divides the stress-strain curve into segments before and after the peak using four coefficients, A, B, C, and D.

$$y = \frac{Ax+Bx^2}{1+Cx+Dx^2} \tag{1}$$

The model and the normalized stress-strain curve of Wang in group C are compared in Fig. 5. The results show that the model not only predicts the rising segment curve well, but also fits well for the falling segment. The good agreement between the experimental results and the model predictions is due to the direct use of the least squares method, which regresses the four parameters A, B, C and D according to the characteristics of each curve. Therefore, the model proposed by Wang can be used to accurately describe the stress-strain curves of ECC with different fiber fit ratios under uniaxial compression conditions in this study.

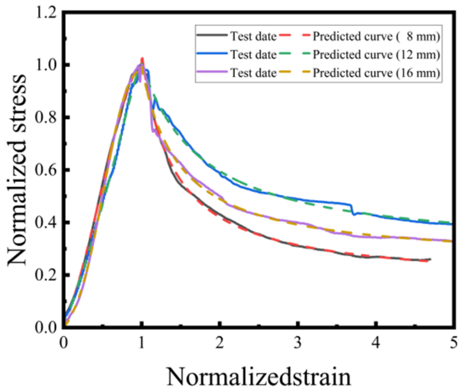

Fig. 5. Fit the results according to Wang's model

The second model is the one by the modified Carreira [7] which also accurately predicts the rising segment of the ECC, and as can be seen in Fig. 6, the falling segment is much more accurate than the previous Carreira's model (with correlation coefficients R^2 ranging from 0.952-0.969). Based on the results of the Group C experiments in this study, the following formulas for k1 and k2 were derived: $k_1 = (60/f_c)^2-0.68$ and $k_2 = (60/f_c)^{1.4}-0.34$.

$$y = \left[\frac{k_1 \beta x}{k_1 \beta - 1 + x^{k_2 \beta}}\right] \tag{2}$$

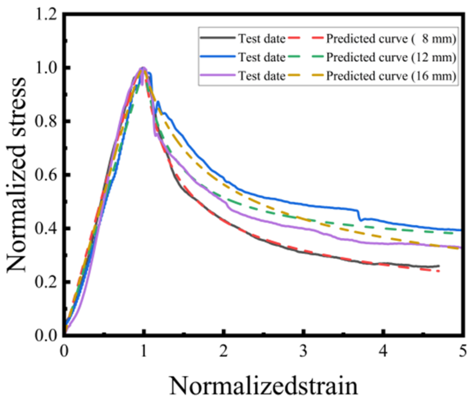

Fig. 6. The fitting results of the modified Carreira's model

Due to the small variation of the rising section of the curve under each fit ratio, Eq. (3) is proposed as a suggested formula for the different fiber lengths and substitution rates out of the comprehensive consideration of the accuracy and convenience of fitting the curve data in this study. The proposed formula simplifies the formula by fixing the variables, and the descending section is controlled by multiple coefficients, which can accurately describe the ECC pressurized descending section curve, and the practicality is greatly improved.

$$y = \begin{cases} 1.304x - 0.304x^2, & 0 \le x \le 1 \\ \frac{Ax+Bx^2}{1+Cx+Dx^2}, & x > 1 \end{cases} \quad (3)$$

4 Conclusion

(1) By observing the damage of the specimen from macro and microscopic perspectives, it is found that the two kinds of fibers bridging each other and the three-dimensional chaotic distribution can inhibit the cracks of different directions and lengths, respectively. At the same time, it is found that the addition of appropriate proportion of POM fiber is conducive to the dispersion of PVA fiber in the cement matrix, thus enhancing the compressive properties, such as the E3 group is 7.4% higher than the A2 group, which is a better performance.

(2) By comparing the compressive strength of each group, it is found that the compressive strength is lower when the two fiber lengths are the same (12 mm), indicating that the hybridization of fibers with different lengths is conducive to the performance of the fibers. Meanwhile, it was found that the compressive strength and modulus of elasticity of each group basically showed a decreasing trend after the replacement rate of 50%. The toughness index basically increases with the increase of fiber length, and the fiber length has little effect on the toughness index when the replacement rate is 50%.

(3) The advantages and disadvantages of the four stress-strain curve models were analyzed, and the fitting effect was compared with the experimental data, on the basis of which the proposed model for the normalized stress-strain curve was given by integrating the simplicity and accuracy considerations.

References

1. Yu K Q, Lu Z D, Dai J G. (2020). Direct Tensile Properties and Stress-Strain Model of UHP-ECC. Journal of Materials in Civil Engineering, 32(1), Article 04019334. https://doi.org/10.1061/(ASCE)MT.1943-5533.
2. Zhou J J, Pan J L, Leung C.K.Y, (2015). Mechanical behavior of fiber-reinforced engineered cementitious compo-sites in uniaxial compression. Journal of materials in civil engineering, 27 (1), 04014111. https://doi.org/10.1061/(ASCE)MT.1943-5533.
3. LOH Z.P.; MO K.H.; TAN C.G. (2019). Mechanical characteristics and flexural behaviour of fibre-reinforced cementitious composite containing PVA and basalt fibres. Indian Academy of Sciences, 44(4), 98. https://doi.org/10.1007/s12046-019-1072-6.

4. Zhang P L, Zeng J Y, Hu J, et al. (2023) Study on compressive mechanical properties and economic performance of steel-PVA hybrid fiber cementitious composites. Silicate Bulletin, 42 (11): 3827-3835. DOI:10.16552/j.cnki.issn1001-1625.2023.11.002.
5. Mansur M.A., Chin M.S., Wee T.H. (1999) Stress-strain relationship of high-strength fiber concrete in compression. Journal of materials in civil engineering, 11 (1), 21–29. https://doi.org/10.1061/(ASCE)0899-1561(1999)11:1(21).
6. Wang P.T., Shah S.P., Naaman A.E. (1978) Stress-strain curves of normal and lightweight concrete in compression. In Journal Proceedings, 75 (11), 603–611. DOI:10.1016/0148-9062(79)90235-3.
7. Carreira D.J., Chu K.H. (1985) Stress-strain relationship for plain concrete in compression. In Journal Proceedings, 82 (6), 797–804. DOI:10.1016/0022-3115(85)90362-9.

Open Access This chapter is licensed under the terms of the Creative Commons Attribution-NonCommercial 4.0 International License (http://creativecommons.org/licenses/by-nc/4.0/), which permits any noncommercial use, sharing, adaptation, distribution and reproduction in any medium or format, as long as you give appropriate credit to the original author(s) and the source, provide a link to the Creative Commons license and indicate if changes were made.

The images or other third party material in this chapter are included in the chapter's Creative Commons license, unless indicated otherwise in a credit line to the material. If material is not included in the chapter's Creative Commons license and your intended use is not permitted by statutory regulation or exceeds the permitted use, you will need to obtain permission directly from the copyright holder.